Theor Chem Acc (2015) 134:140
DOI 10.1007/s00214-015-1752-1

REGULAR ARTICLE

Theoretical studies of traditional and halogen-shared halogen bonds: the doped all-metal aromatic clusters MAl_3^- (M = Si, Ge, Sn, Pb) as halogen bond acceptors

Na Cheng[1] · Yongjun Liu[1,2] · Changqiao Zhang[1]

Received: 6 July 2015 / Accepted: 22 October 2015 / Published online: 31 October 2015

Abstract In this paper, ab initio MP2 calculations have been performed to study the traditional and halogen-shared halogen bonds formed by a series of doped all-metal aromatic clusters MAl_3^- (M = Si, Ge, Sn, Pb) and YX (Y = HCC–, F_3C–, HO–; X = Cl, Br, I). On the basis of our calculations, four halogen-bonded interaction modes, coded as MAl_3^-–XY-**1**, MAl_3^-–XY-2, MAl_3^-–XY-**3** and MAl_3^-–XY-**4**, have been recognized for complexes of MAl_3^-–XY. In particular, the configurations (configurations **2** and **3**) of the HCCX- and F_3CX-containing complexes display different arrangements from those of HOX-containing complexes. Although the most positive electrostatic potentials on the surfaces of X atoms in monomers of YX (Y = HCC–, F_3C–, HO–; X = Cl, Br, I) are similar, the interaction strength of HOX-containing complex is much stronger than those of HCCX- and F_3CX-containing complexes. Based on the AIM, NBO and ELF analyses, the halogen bonds in the HCCCl/Br- and F_3CCl/Br-containing complexes belong to traditional halogen bonds, while those in $SiAl_3^-$–$BrCF_3$-**1**, $GeAl_3^-$–$BrCF_3$-**1** and HCCI- and F_3CI-containing complexes are halogen-shared halogen bonds. The halogen bonds in the HOX-containing complexes belong to covalent bonds or halogen-shared halogen bonds.

Keywords Halogen bonds · Hydrogen bonds · MP2 · AIM analysis · Aromatic clusters MAl_3^-

1 Introduction

Hydrogen bonds have been proved to play important roles in molecular biology, material science and supramolecular chemistry [1–3]. Recently, another type of intermolecular interaction named as halogen bonds attracted much attention [4–6]. Halogen bonds are a kind of noncovalent interaction between a covalently bound halogen atom X (X = F, Cl, Br, I) and the negative site of another molecule. Politzer et al. [7] have illuminated the formation of halogen bonds with the electrostatic potential of covalently bound halogen atoms. They recognized that the covalent halogen atom possesses a positive electrostatic potential region called σ-hole along the extension of the C–X bond, which is responsible for forming halogen bonds. Numerous studies have indicated that the halogen bonds compete with the hydrogen bonds, but the halogen bonds exhibit a better directionality [8–10]. Of course, the halogen bonds also share some similarities with the hydrogen bonds [11, 12], such as the binding strength and driven force.

So far, a number of theoretical and experimental studies have been conducted for understanding the structure, stability and nature of halogen bonds [7, 13–20]. In the conventional halogen bonds, the halogen bond acceptors are those containing lone pair electrons, such as fluorine, oxygen and nitrogen, or those containing π electrons, such as ethylene and benzene [15, 17, 20–26]. It should be

Electronic supplementary material The online version of this article (doi:10.1007/s00214-015-1752-1) contains supplementary material, which is available to authorized users.

✉ Yongjun Liu
yongjunliu_1@sdu.edu.cn

✉ Changqiao Zhang
zhangchqiao@sdu.edu.cn

[1] School of Chemistry and Chemical Engineering, Shandong University, Jinan 250100, Shandong, China

[2] Key Laboratory of Tibetan Medicine Research, Northwest Institute of Plateau Biology, Chinese Academy of Sciences, Xining 810001, Qinghai, China

noted that hypohalous acids (HOX, X = F, Cl, Br, I) are very interesting compounds, in which the σ-inductive role of the halogen atoms interplays with the repulsive interaction formed by the lone pairs of the adjacent oxygen and halogen atoms, making them have unique bonding characteristics, i.e., the O–F bond is a covalent and polarized one, whereas the bonding between O and Cl, Br and I atoms is of the electron donor–acceptor type with the halogen atoms donating the electron density to the valence shell of oxygen [27]. In 2009, Blanco et al. [28] found that hypohalous acids can form two halogen-bonded complexes, two hydrogen-bonded complexes and two van der Waals complexes with carbon monoxide. Recently, Li et al. [29] studied the H···O and X···O contacts in complexes of hypohalous acids (HOX, X = F, Cl, Br) with formaldehyde at the MP2/aug-cc-pVTZ'' computational level.

About 20 years ago, Robinson and co-workers synthesized some stable organometallic compounds that contain a cyclic Ga_3 [30], and in 2001, Li et al. [31] further prepared a series of all-metal systems, such as Al_4^{2-} dianion and ionic clusters MAl_3^- (M = Li, Na or Cu), which were proved to have partial aromatic character. Recently, it has been demonstrated by Li et al. [32] that the all-metal Al_4^{2-} can also form halogen bonds with the covalent halogen atoms of halohydrocarbons X–R (X = Cl, Br, I; R=H_3C–, H_5C_2–, H_2C=HC–, HC≡C–), confirming that the all-metal aromatic ring Al_4^{2-} can also act as a halogen bond acceptor.

In addition, experimental and theoretical studies showed that the doped all-metal rings MAl_3^- (M = Si, Ge, Sn, Pb) also show aromaticity [33]. But the geometries and electric properties of Al_4^{2-} and MAl_3^- are significantly different [31, 33]. For Al_4^{2-}, its geometry is a standard square and the two p electrons delocalize evenly over the four Al atoms. However, for each of the doped all-metal aromatic clusters MAl_3^- (M = Si, Ge, Sn, Pb), both a four-membered heterocyclic structure (C_{2v}) and a pyramidal structure (C_{3v}) were recognized, but the most stable structure is the C_{2v} cyclic one. Moreover, the calculated molecular orbitals showed that, due to the substitution of Al by Si, Ge, Sn and Pb, the delocalization of the two p electrons exhibits different features. For example, in $SiAl_3^-$, the delocalized π orbital is HOMO-1, which is heavily concentrated at the Si site. However, for $GeAl_3^-$, $SnAl_3^-$ and $PbAl_3^-$, the delocalized π orbitals (HOMO) steadily expand toward the terminal Al atom. Therefore, we can speculate that if the clusters MAl_3^- (M = Si, Ge, Sn, Pb) form halogen-bonded complexes with the covalently bound halogen atoms, the halogen bonds will exhibit different characteristics, and the doped atoms may impose different influences on the strength and nature of halogen bonds. To confirm these conjectures, in this article, three simple compounds with different types of covalent halogen atoms, HCCX, F_3CX and hypohalous acids HOX (X = Cl, Br, I), were selected as halogen bond donors and the doped clusters MAl_3^- (M = Si, Ge, Sn, Pb) with C_{2v} cyclic structures were used as halogen bond acceptors to study the structures, characteristics and nature of halogen bonds in the complexes of MAl_3^-–YX (M = Si, Ge, Sn, Pb; Y=HCC–, F_3C–, HO–; X=Cl, Br, I) by using Moller–Plesset second-order perturbation (MP2) calculations.

2 Computational methods

Since the Moller–Plesset second-order perturbation (MP2) method has been proved to be successful in predicting the characteristics and nature of intermolecular interactions, such as hydrogen bonds and halogen bonds [24–26, 28, 29, 32, 34], in this work, the geometries of all halogen-bonded and hydrogen-bonded complexes were fully optimized by using MP2 method in conjugation with Dunning's basis set aug-cc-pVTZ'', as implemented in Gaussian 09 [35]. The basis set aug-cc-pVTZ'' represents that the aug-cc-pVTZ basis set was adopted for H, C, O, F, Al, Si, Cl, Br and Ge atoms, while the aug-cc-pVTZ-PP basis set was used for I, Sn and Pb atoms [36, 37]. The basis set superposition error (BSSE) was eliminated utilizing the counterpoise correction method of Boys and Bernardi [38]. For the halogen-bonded complexes MAl_3^-–XY (M = Si, Ge, Sn, Pb; X = Cl, Br, I; Y = HCC–, F_3C–, HO–) and hydrogen-bonded complexes $SiAl_3^-$–HOCl, the geometry optimizations were carried out with the BSSE-corrected energy expression. Normal mode vibrational frequency calculations were performed at the same computational level to affirm whether the optimized structures are stable stationary points at the local potential energy surface. The natural bond orbital (NBO) analysis was performed at the MP2/aug-cc-pVTZ'' level using the Gaussian 09 NBO package [39]. The electrostatic potentials of the monomers were calculated using Gaussian 09. Based on the Bader's atoms in molecules (AIM) theory [40], AIM calculations were performed for bond critical points in all selected complexes at the MP2/aug-cc-pVTZ'' level using the AIMAll program [41]. The topological analysis of the electron localization function (ELF) was performed by Multiwfn 3.1 suite of program [42, 43].

3 Results and discussion

3.1 Halogen bonds

3.1.1 Geometrical parameters and interaction energies

The calculated electrostatic potential surface of $SiAl_3^-$ is shown as an example in Fig. 1. Due to the symmetry of

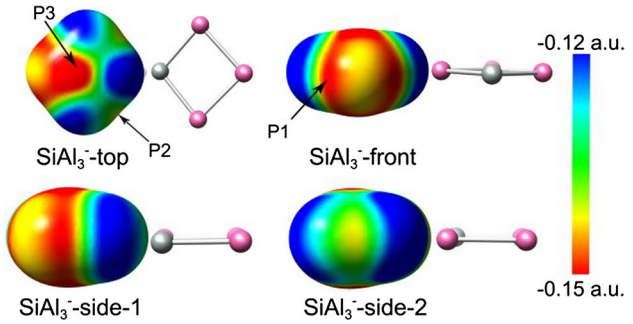

Fig. 1 Computed electrostatic potentials on the 0.001 a.u. molecular surfaces of the halogen bond acceptor $SiAl_3^-$. Silicon and aluminum atoms are represented in *light gray* and *pink*, respectively

$SiAl_3^-$, three pairs of local minimum points of electrostatic potential are found, namely P1, P2 and P3, respectively. P1 is located between the bonded Si and Al atoms, while P2 is located in the middle of the two bonded Al atoms. P3 is situated in the upper center of the square. The values of the most negative electrostatic potentials of MAl_3^- are given in Table 1. The most negative electrostatic potentials at P1, P2 and P3 sites have the similar tendencies, i.e., P2 corresponds to the most negative electrostatic potential while P3 to the least negative electrostatic potential. With the M atom changing from Si to Pb, the absolute values of the largest negative electrostatic potentials only decrease slightly. In general, the most negative electrostatic potentials of the doped MAl_3^- (−87 to −99 kcal mol^{-1}) are much larger than those of Al_4^{2-} (−160 to −168 kcal mol^{-1}).

The molecular electrostatic potential maps at the 0.001 a.u. isosurface of the electron density of monomers YX (Y = HCC–, F_3C–, HO–; X = Cl, Br, I) were also calculated at the MP2/aug-cc-pVTZ'' level, which are shown in Fig. 2. Not surprisingly, all the electrostatic potentials on the covalent X atoms are anisotropic, and the regions of the positive electrostatic potential, σ-hole, of halogen donors are centered on the extension of the C–X or O–X bond. The values of the most positive electrostatic potentials of monomers YX are also listed in Table 1. Among the monomers of HCCX, F_3CX and HOX, the σ-holes of HOX are calculated to be the most positive sites. Moreover, with the X atom changing from Cl to I, the values of the most positive electrostatic potentials on X atoms increase gradually.

Figure 3 shows the optimized geometries of the Cl complexes, and Figures S1 and S2 display those of Br and I complexes, respectively. For a convenient and clear illustration, four types of halogen-bonded complexes are, respectively, denoted as MAl_3^-–XY-**1** (M = Si, Ge, Sn, Pb), $SiAl_3^-$–XY-**2**, $SiAl_3^-$–XY-**3** and $SiAl_3^-$–XY-**4** (X = Cl, Br, I; Y = HCC–, F_3C–, HO–). In order to explore how the doped atoms will influence the strength and nature of halogen bonds, we select configuration **1** of non-$SiAl_3^-$ clusters to optimize and analyze. It should be noted that the arrangements of complexes $SiAl_3^-$–XY-**2** and $SiAl_3^-$–XY-**3** (X = Cl, Br, I; Y = HCC–, F_3C–) are different from those of complexes $SiAl_3^-$–XOH-**2** and $SiAl_3^-$–XOH-**3**, as shown in Figs. 3, S1 and S2. For complexes $SiAl_3^-$–XY-**2** and $SiAl_3^-$–XY-**3** (Y = HCC–, F_3C–; X = Cl, Br, I), YX binds with $SiAl_3^-$ at the P1 and P2 sites and the structures of halogen-bonded complexes are similar to those formed by Al_4^{2-} and halohydrocarbon [32]. However, $SiAl_3^-$ prefers to interact with HOX at the corner sites (Al atoms) for complexes $SiAl_3^-$–XOH-**2** and $SiAl_3^-$–XOH-**3**. Meanwhile, we also find that the corresponding complexes $SiAl_3^-$–$BrCF_3$-**2**, $SiAl_3^-$–ICCH-**2** and $SiAl_3^-$–ICF_3-**2** were not recognized. The reason may be that their interactions are extremely weak relative to the interactions in complexes $SiAl_3^-$–ICCH-**1** and $SiAl_3^-$–ICF_3-**1** (11.45 and 13.56 kcal mol^{-1} for complexes $SiAl_3^-$–ICCH-**1** and $SiAl_3^-$–ICF_3-**1**, respectively). In addition, frequency calculations reveal that complexes MAl_3^-–ClCCH-**1** (except $PbAl_3^-$–ClCCH-**1**), MAl_3^-–$ClCF_3$-**1**, $PbAl_3^-$–BrCCH-**1**, $PbAl_3^-$–ICCH-**1**, $PbAl_3^-$–$BrCF_3$-**1** and $PbAl_3^-$–ICF_3-**1** correspond to very small imaginary frequencies (<10*i*); even these complexes were re-optimized with the more tight convergence criteria, which means they are not true local energy minima.

Table 1 The most positive electrostatic potential (V_{max}, kcal mol^{-1}) on surface of X atom in YX (Y = HCC–, F_3C–, HO–; X = Cl, Br, I) and the most negative electrostatic potential (V_{min}, kcal mol^{-1}) of the MAl_3^- (M = Si, Ge, Sn, Pb)

Monomer	V_{max}	Monomer	V_{max}	Monomer	V_{max}
HCCCl	23.8	HCCBr	29.2	HCCI	37.5
F_3CCl	24.3	F_3CBr	28.7	F_3CI	36.6
HOCl	26.1	HOBr	34.1	HOI	49.9
Monomer	V_{min}				
	P1	P2	P3		
$SiAl_3^-$	−94.5	−89.6	−98.9		
$GeAl_3^-$	−94.0	−89.3	−98.3		
$SnAl_3^-$	−90.8	−87.6	−96.0		
$PbAl_3^-$	−89.3	−87.5	−95.4		

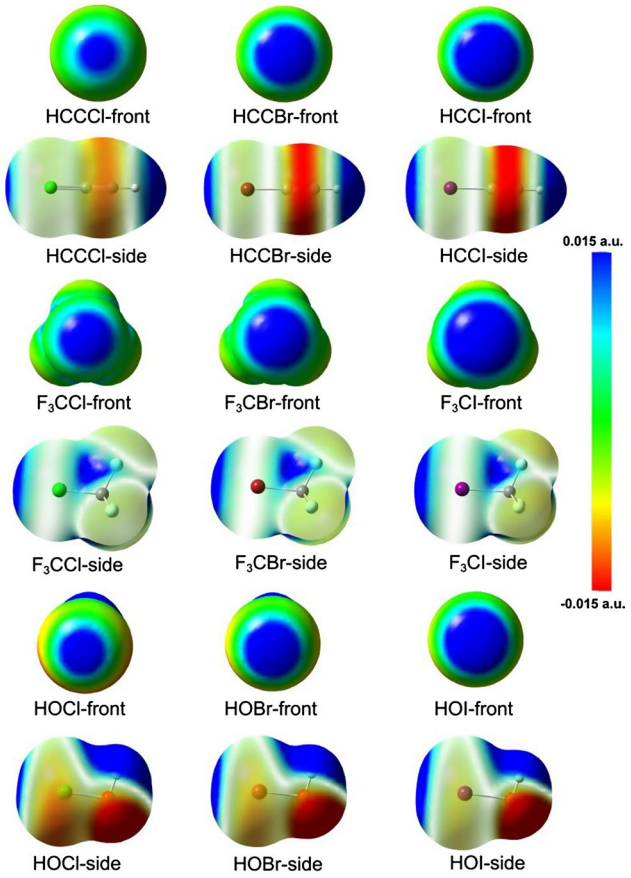

Fig. 2 Computed electrostatic potentials on the 0.001 a.u. molecular surfaces of the halogen bond donors

For the Cl complexes, bond lengths (R) between Cl and Al/M (M = Si, Ge, Sn, Pb), bond length of C/O–Cl, changes in bond lengths (Δr) of C–Cl and O–Cl and BSSE-corrected interaction energies (ΔE^{cp}) are listed in Table 2. For HCCCl- and F_3CCl-containing complexes, bond lengths R fall in the range of 3.500–3.900 Å, which are clearly smaller than the sum (about 4.5 Å) of van der Waals radii of Al and X atoms [32]. In addition, the changes in bond lengths of C–Cl exhibit different characters. For example, in the HCCCl-containing complexes, the bond lengths of C–Cl are elongated by ~0.003 Å, whereas those in the F_3CCl-containing complexes are shortened by ~0.01 Å. These imply that the HCCCl- and F_3CCl-containing complexes are formed by traditional halogen bonds with long M/Al–Cl and short C–Cl distances, which belong to pure closed-shell interaction. However, in the HOCl-containing complexes, all bond lengths R are shorter than 3.0 Å, and they are longer than their corresponding chemical bonds by ~0.3 Å (the lengths of covalent bonds of Si–Cl, Ge–Cl, Sn–Cl and Pb–Cl are 2.02, 2.10, 2.33 and 2.42 Å, respectively). They imply that the halogen bond between MAl_3^- and HOCl is extremely strong. Moreover, in the HOCl-containing complexes, the O–Cl bonds are greatly weakened with their bond lengths increased more than 0.30 Å. In short, all the HOCl-containing complexes are stabilized by chlorine-shared [44] halogen bonds, which belong to closed-shell interaction with short M/Al–Cl and long O–Cl distances.

Table S1 in supporting information presents some geometrical and energetic characteristics of the Br and I complexes. For MAl_3^-–Br/ICCH and MAl_3^-–Br/ICF_3 complexes, the bond lengths R are longer than 3.0 Å; meanwhile, the bond lengths R in complexes MAl_3^-–Br/IOH are shorter than 3.1 Å. Table 2 and Table S1 also show that, with the increase in X atomic numbers, the bond lengths (R) in the HCCX- and F_3CX-containing complexes decrease gradually, whereas the bond lengths (R) in HOX-containing complexes increase gradually. In addition, in the HCCX-containing complexes, the bond lengths of C–X are elongated and the changes in C–X are increased following the order of X = Cl < Br < I. However, the reverse order is found for the HOX-containing complexes. With X changing from Cl to I, the changes in C–X display different characteristics in F_3CX-containing complexes. In F_3CX-containing complexes, the bond lengths of C–Cl are shortened and those of C–Br/I are elongated. The bond lengths (R) in all selected complexes follow the order of Si < Ge < Sn < Pb. In a word, for the HCCX- and F_3CX-containing complexes, with the increase in the X atomic number, halogen bonds change from the traditional halogen bonds to the halogen-shared halogen bonds.

The BSSE-corrected interaction energies (ΔE^{CP}) calculated at the MP2/aug-cc-pVTZ'' level are listed in Table 2 and Table S1. One can see from Table 2 that the HOCl-containing complexes correspond to the most negative interaction energies, which are much smaller than those of the F_3CCl- and HCCCl-containing complexes. For the HOCl-containing complexes, all the interaction energies are smaller than −14.0 kcal mol^{-1}. However, all interaction energies between MAl_3^- and HCCCl or F_3CCl are larger than −6.0 kcal mol^{-1}. These differences may be attributed to the different nature of these halogen bonds. In HCCCl- and F_3CCl-containing complexes, the halogen bonds are traditional halogen bonds which belong to pure closed-shell interactions, while in complexes MAl_3^-–ClOH, the interactions between Cl and the atoms Al/M (M = Si, Ge, Sn, Pb) exhibit partial covalent bond characteristic and belong to closed-shell interactions, which will be discussed in detail in the following sections.

Table 2 shows that, in $SiAl_3^-$–ClCCH-**1**, $SiAl_3^-$–ClCCH-**2**, $SiAl_3^-$–ClCCH-**3** and $SiAl_3^-$–ClCCH-**4** complexes the interaction energies are calculated to be −3.99, −4.19, −3.67 and −4.98 kcal mol^{-1}, respectively. One can see that the halogen-bonded interaction strength in complex $SiAl_3^-$–ClCCH-**3** is the weakest and

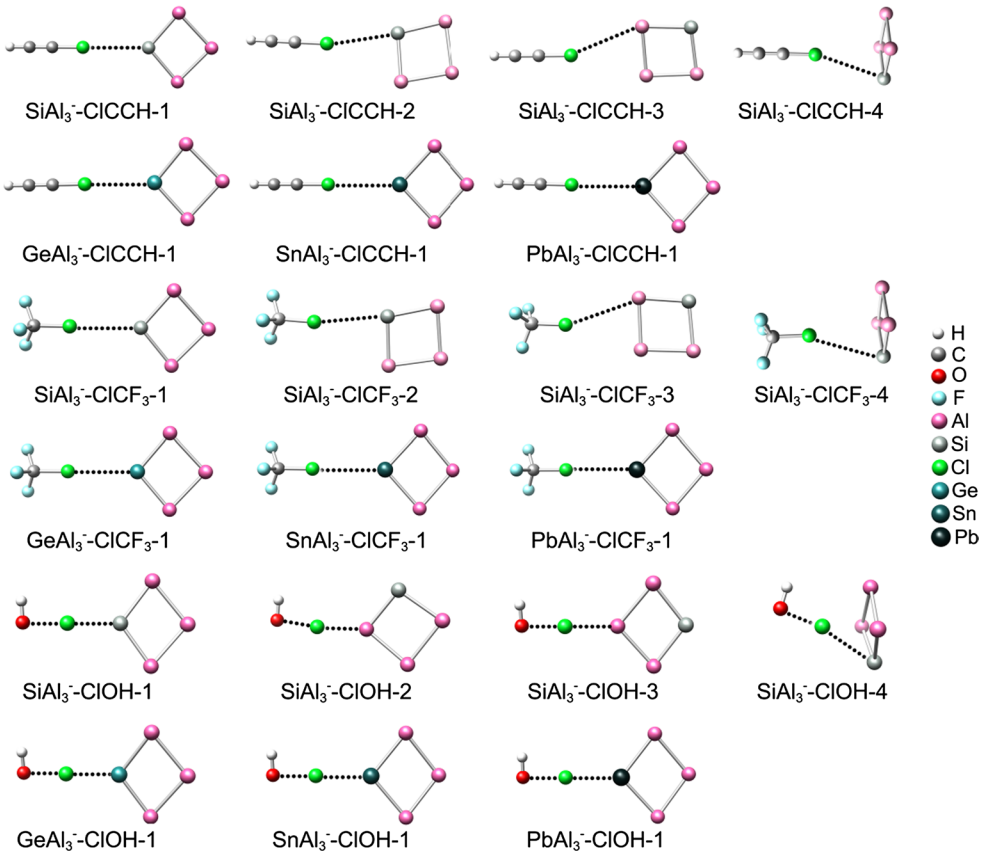

Fig. 3 The optimized structures of the Cl complexes

the interaction in complex $SiAl_3^-$–ClCCH-**4** is the strongest among the HCCCl-containing complexes. Besides, Table 2 also shows that the influence of doped M atoms is minor for complexes MAl_3^-–ClCCH-**1**. The interaction energy is ~−3.99 kcal mol^{-1} for both complexes $SiAl_3^-$–ClCCH-**1** and $GeAl_3^-$–ClCCH-**1**, and they are −3.42 and −3.28 kcal mol^{-1} for complexes $SnAl_3^-$–ClCCH-**1** and $PbAl_3^-$–ClCCH-**1**, respectively. These results indicate that the doped M atoms have little influence on the interaction energy of the HCCCl-containing complex. Because the interaction modes in complexes MAl_3^-–$ClCF_3$ are the same as those in complexes MAl_3^-–ClCCH, the changes in the interaction energies are similar. But the interaction energies of the complexes $SiAl_3^-$–ClOH display different trends. Table 2 shows that the interaction strengths among the four complexes $SiAl_3^-$–ClOH follow the order of $SiAl_3^-$–ClOH-**1** < $SiAl_3^-$–ClOH-**3** < $SiAl_3^-$–ClOH-**2** < $SiAl_3^-$–ClOH-**4**. The interaction energy of complex MAl_3^-–ClOH-1 is decreased following the order of Si < Ge < Sn < Pb. When the doped M atom changes from Si to Pb, the interaction energy decreases by 6.30 kcal mol^{-1}.

As shown in Table S1, similar results are also observed for the interaction energies of halogen bonds though the interaction energies of Br and I complexes are more negative than those of the Cl complexes. For HCCX- and F_3CX-containing complexes, the interaction strength increases about three times from Cl to I. But for HOX-containing complexes, with the increase in X atomic number, the interaction energies of complexes MAl_3^-–XOH-**1** and $SiAl_3^-$–XOH-**4** increase gradually. But for $SiAl_3^-$–XOH-**2** and $SiAl_3^-$–XOH-**3** complexes, the interaction energies only change slightly. Thus, when X is I atom, the difference in interaction energies between complexes $SiAl_3^-$–IOH-**1**, $SiAl_3^-$–IOH-**2** and $SiAl_3^-$–IOH-**3** is very small. This means that other kinds of interactions except the electrostatic interaction are also responsible for the formation of MAl_3^-–XOH complexes.

To investigate the change in aromaticity of MAl_3^- units in forming halogen-bonded complexes, nuclear independent chemical shift NICS(0) in the center of MAl_3^- units is calculated at the B3LYP/aug-cc-pVTZ" level. The calculated NICS(0) values of MAl_3^- are ~−36.0 (NICS(0): −36.0 for $SiAl_3^-$, −36.1 for $GeAl_3^-$, −35.6 for $SnAl_3^-$ and −35.7 for $PbAl_3^-$), which are similar to those of Al_4^{2-} unit (−36.5) [28]. The NICS(0) values of MAl_3^- units in the Cl complexes are listed in Table S2. One can see that, in the HCCCl- and F_3CCl-containing complexes, the NICS(0) values have a little change (<1.0). However, in the HOCl-containing complexes, the NICS values show a change of ~2.0 to 6.0. These results indicate that the electrostatic interaction has minor influence on the aromaticity

Table 2 Bond length (R, Å) between Cl and Al/M (M = Si, Ge, Sn, Pb), bond length of C/O–Cl ($r_{C/O-Cl}$), change in bond length (Δr, Å) of C/O–Cl bonds and BSSE-corrected interaction energies (ΔE^{cp}, kcal mol^{-1}) of the Cl complexes

Complex	R	$r_{C/O-Cl}$	Δr	ΔE^{CP}
$SiAl_3^-$–ClCCH-**1**	3.482	1.642	0.003	−3.99
$SiAl_3^-$–ClCCH-**2**	3.529	1.642	0.003	−4.19
$SiAl_3^-$–ClCCH-**3**	3.883	1.642	0.003	−3.67
$SiAl_3^-$–ClCCH-**4**	3.731	1.644	0.005	−4.98
$GeAl_3^-$–ClCCH-**1**	3.495	1.642	0.003	−3.99
$SnAl_3^-$–ClCCH-**1**	3.704	1.642	0.003	−3.42
$PbAl_3^-$–ClCCH-**1**	3.706	1.641	0.002	−3.28
$SiAl_3^-$–$ClCF_3$-**1**	3.455	1.740	−0.011	−4.64
$SiAl_3^-$–$ClCF_3$-**2**	3.569	1.738	−0.013	−4.80
$SiAl_3^-$–$ClCF_3$-**3**	3.893	1.740	−0.011	−4.21
$SiAl_3^-$–$ClCF_3$-**4**	3.731	1.742	−0.009	−5.57
$GeAl_3^-$–$ClCF_3$-**1**	3.469	1.741	−0.010	−4.62
$SnAl_3^-$–$ClCF_3$-**1**	3.682	1.742	−0.009	−3.98
$PbAl_3^-$–$ClCF_3$-**1**	3.686	1.742	−0.009	−3.82
$SiAl_3^-$–ClOH-**1**	2.403	2.023	0.326	−20.34
$SiAl_3^-$–ClOH-**2**	2.396	2.029	0.332	−27.34
$SiAl_3^-$–ClOH-**3**	2.416	2.032	0.335	−24.19
$SiAl_3^-$–ClOH-**4**	2.851	2.007	0.310	−27.95
$GeAl_3^-$–ClOH-**1**	2.475	2.024	0.327	−17.95
$SnAl_3^-$–ClOH-**1**	2.635	2.040	0.343	−16.73
$PbAl_3^-$–ClOH-**1**	2.709	2.063	0.366	−14.03

of MAl_3^-, but the orbital interaction can influence the aromaticity of MAl_3^- to some extent.

3.1.2 NBO and AIM analyses

To understand the interaction nature in the selected complexes, the NBO analysis was performed at the MP2/aug-cc-pVTZ'' level. The results of NBO analysis indicate that the nature of halogen bonds in the HCCX- and F_3CX-containing complexes is different from that in the HOX-containing complexes. In the HCCX- and F_3CX-containing complexes, the covalent bonds were not found between Al/M and X atoms. However, in the HOX-containing complexes, the original O–X bonds in the monomers of HOX have been broken and new Al/M–X bonds have been formed. This is because the O–X (X = Cl, Br, I) bonds are of donor–acceptor type with halogen atom donating the electron density to the oxygen valence shell. In addition, according to the NBO analysis, the charge transfers between the monomers, orbital interactions and the corresponding second-order perturbation stabilization energies of the Cl, Br and I complexes are listed in Tables S3, S4 and S5, respectively. From Table S3, one can see that, due to the formation of Al/M-Cl bonds in complexes MAl_3^-–ClOH, the donor–acceptor orbital interactions in complexes MAl_3^-–ClOH display different characteristics with those in complexes MAl_3^-–ClCCH and MAl_3^-–$ClCF_3$. In complexes MAl_3^-–ClOH, the dominant orbital interaction is $n_O \rightarrow \sigma^*_{M/Al-Cl}$, which corresponds to very large stabilization energies (72–125 kcal mol^{-1}). It indicates that the orbital interaction plays a significant role in the interaction between O and Cl atoms. However, in complexes MAl_3^-–ClCCH and MAl_3^-–$ClCF_3$, all the charge transfers and stabilization energies are very small, implying the orbital interactions between the acceptor and donor being very weak. By comparing the stabilization energies in Table S3 and the interaction energies in Table 2, we found that these two items have no direct correlation, which suggests that the orbital interaction does not play a dominate role in forming halogen bonds in these HCCCl- and F_3CCl-containing complexes.

With regard to complexes MAl_3^-–BrOH and MAl_3^-–IOH, Tables S4 and S5 show that the dominant orbital interactions are also $n_O \rightarrow \sigma^*_{M/Al-Br/I}$. However, in the HCCX- and F_3CX-containing complexes, with the increase in X atomic number, the stabilization energies of the dominant orbital interaction increase gradually. Accompanied by the orbital interactions between the two monomers, there is a charge transfer from the halogen acceptor to the donor. In addition, charge transfer also increases gradually in the order of X = Cl < Br < I. These indicate that the contribution of orbital interaction to the formation of halogen bonds increases in forming the Cl to I complexes. For HCCX- and F_3CX-containing complexes, the largest electron density transfer was found between the Al–Si/Al bonding σ orbital and the C–X antibonding σ* orbital in configurations **2** and **3** and between lone electron pair(s) of Si and the C–X antibonding σ* orbital in configuration **4**, whereas the largest electron density transfer in configuration I exhibits different features. For configuration **1**, the dominant orbital interaction is $\sigma_{Al\text{-}Si} \rightarrow \sigma^*_{C-Cl/Br}$ in the Cl and Br complexes that contain $SiAl_3^-$ unit and $n_M \rightarrow \sigma^*_{C-I}$ in the Cl and Br complexes that contain non-$SiAl_3^-$ and all I complexes.

AIM topological analysis has been proved to be a useful tool in understanding the nature and properties of noncovalent interactions, such as hydrogen bond, halogen bond and pnicogen bond [45, 46]. Figure 4 shows the molecular graphs of complexes formed by MAl_3^- (M = Si, Ge, Sn, Pb) clusters and YCl (Y = HCC–, F_3C–, HO–). One can see that the halogen bonds exist in all complexes MAl_3^-–ClY, which can be also evidenced by the bond critical points (BCPs) between Cl and M/Al atoms. The analysis of BCPs provides information on the nature of interatomic interaction. Therefore, we analyze the electron density (ρ_b), Laplacian of electron density ($\nabla^2\rho_b$), local potential energy density (V_b), local kinetic energy (G_b) and total energy density ($H_b = V_b + G_b$) of the BCPs. The BCPs properties

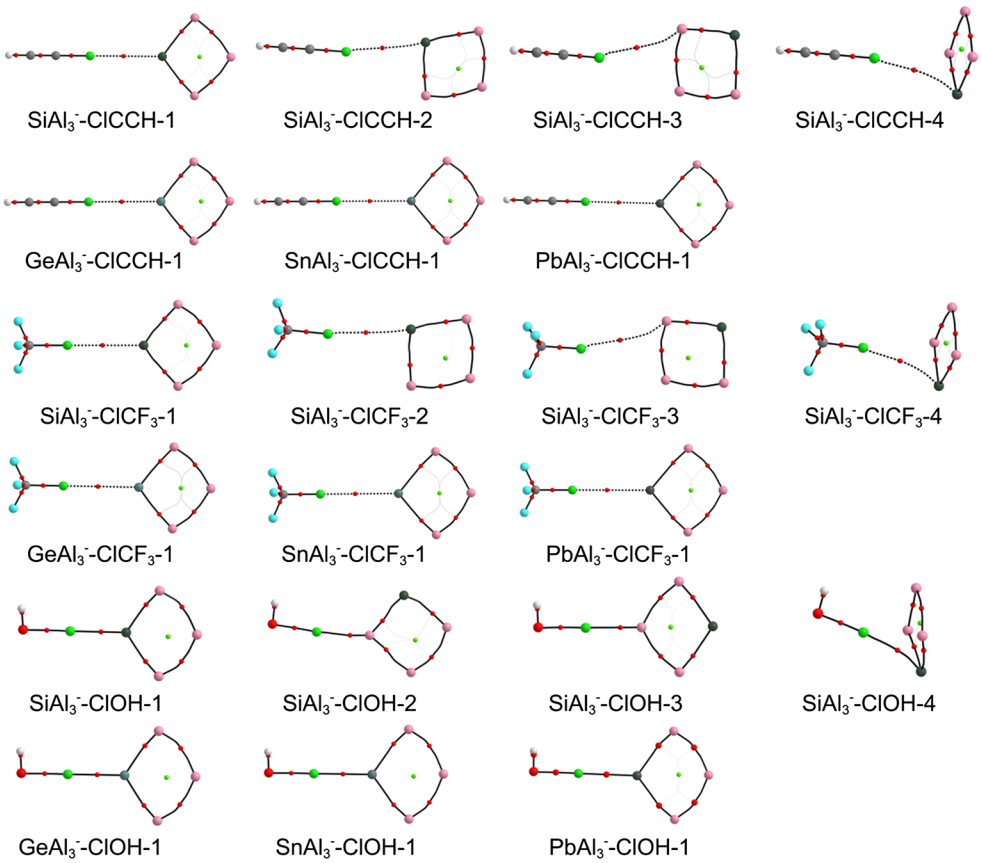

Fig. 4 The molecular graphs of the Cl complexes. *Small red dots* indicate the bond critical points, and *small green dots* denote the ring critical points in cyclic structures

of the Cl–Al/M (M = Si, Ge, Sn, Pb) and O–Cl bonds in the Cl complexes calculated at the MP2/aug-cc-pVTZ" level are listed in Table 3. Tables S6 and S7 give the BCPs properties of the X-Al/M and O–X bonds in the Br and I complexes, respectively. In general, the type of interaction can be characterized by the sign of $\nabla^2\rho_b$. For van der Waals interactions, ionic contacts and hydrogen and halogen bonds, the sign of $\nabla^2\rho_b$ is positive owing to the depletion of electron charge within the atom–atom region. For the covalent and polarized bonds, due to the centralization of electron charge within the atom–atom region, the $\nabla^2\rho_b$ is negative. In a word, the interaction in the region of $\nabla^2\rho_b < 0$ belongs to a shared-shell interaction and that of $\nabla^2\rho_b > 0$ is a closed-shell interaction. Usually, $\nabla^2\rho_b$ is positive, as in most hydrogen and halogen bonds; however, there are also cases where $\nabla^2\rho_b$ is negative. In these cases, the hydrogen and halogen bonds are very strong, such as H···O in $H_5O_2^+$ [47] and Br···F^- in PhBr-F^- [48]. They are typical examples that covalent characters exist in strong hydrogen and halogen bonds. Moreover, Cremer and Kraka [49] found that the Laplacian values are positive at BCPs for covalent double and triple CO bonds, which implies that the sign of Laplacian is not a satisfactory indicator for the classification of interactions. Therefore, they proposed that it is more appropriate to characterize character of a bond by using the values of ρ_b and the sign of $\nabla^2\rho_b$ and H_b. When $H_b > 0$, a bond is mainly an electrostatic interaction; if $H_b < 0$, the interaction exhibits the covalent nature owing to the electron stabilization at BCPs. Later, the ratio $|V_b|/G_b$ was used to characterize the nature of interaction [50]. Consequently, if $\nabla^2\rho_b > 0$, $H_b > 0$ and $|V_b|/G_b < 1$, a bond is a pure closed-shell interaction; if $\nabla^2\rho_b > 0$, $H_b < 0$ and $1 < |V_b|/G_b < 2$, the bond has a partial covalent nature and belongs to closed-shell interaction; when $\nabla^2\rho_b < 0$, $H_b < 0$ and $2 < |V_b|/G_b$, the bond is a typical covalent interaction.

As shown in Tables 3, S6 and S7, for the HCCX- and F_3CX-containing complexes, both the parameters of ρ_b and $\nabla^2\rho_b$ are positive and their values are very small. The values of ρ_b are within the range of 0.002–0.035 a.u., which is a topological criterion proposed by Koch and Popelier [51] for assessing the existence of hydrogen bonds. Besides, the Cl complexes have $H_b > 0$ and $|V_b|/G_b < 1$. All these indicate that the halogen bonds are pure closed-shell interaction in the Cl complexes. The H_b values of halogen-bonded BCPs of I complexes are negative, and they are very small (−0.0005 to −0.0055 a.u.). The I complexes have $1 < |V_b|/G_b < 2$. These indicate that, compared to those in the Cl complexes, the halogen bonds of I complexes belong to closed-shell interactions with slight covalent characteristic. Besides, in the Br complexes, the $SiAl_3^-$–$BrCF_3$-**1**

Table 3 Some bond critical point properties (in a.u.) of the Cl···O and Cl···Al/M (M = Si, Ge, Sn, Pb) in studied complexes at MP2/aug-cc-pVTZ" level

Complex		ρ_b	$\nabla^2\rho_b$	V_b	G_b	$\lvert V_b\rvert/G_b$	H_b
$SiAl_3^-$–ClCCH-**1**	Cl···M	0.0091	0.0225	−0.0042	0.0049	0.8571	0.0007
$SiAl_3^-$–ClCCH-**2**		0.0074	0.0207	−0.0032	0.0042	0.7619	0.0010
$SiAl_3^-$–ClCCH-**3**		0.0057	0.0134	−0.0020	0.0027	0.7407	0.0007
$SiAl_3$-ClCCH-**4**		0.0068	0.0152	−0.0026	0.0032	0.8125	0.0006
$GeAl_3^-$–ClCCH-**1**		0.0085	0.0235	−0.0040	0.0049	0.8163	0.0009
$SnAl_3^-$–ClCCH-**1**		0.0072	0.0190	−0.0030	0.0039	0.7692	0.0009
$PbAl_3^-$–ClCCH-**1**		0.0070	0.0198	−0.0031	0.0040	0.7750	0.0009
$SiAl_3^-$–$ClCF_3$-**1**		0.0092	0.0241	−0.0042	0.0051	0.8235	0.0009
$SiAl_3^-$–$ClCF_3$-**2**		0.0078	0.0210	−0.0034	0.0043	0.7907	0.0009
$SiAl_3^-$–$ClCF_3$-**3**		0.0058	0.0131	−0.0020	0.0026	0.7692	0.0006
$SiAl_3^-$–$ClCF_3$-**4**		0.0072	0.0152	−0.0025	0.0032	0.7813	0.0007
$GeAl_3^-$–$ClCF_3$-**1**		0.0092	0.0239	−0.0043	0.0051	0.8431	0.0008
$SnAl_3^-$–$ClCF_3$-**1**		0.0077	0.0192	−0.0032	0.0040	0.8000	0.0008
$PbAl_3^-$–$ClCF_3$-**1**		0.0075	0.0200	−0.0032	0.0041	0.7805	0.0009
$SiAl_3^-$–ClOH-**1**		0.0603	−0.0091	−0.0479	0.0228	2.1009	−0.0251
$SiAl_3^-$–ClOH-**2**		0.0405	0.0886	−0.0422	0.0322	1.3106	−0.0100
$SiAl_3^-$–ClOH-**3**		0.0402	0.0705	−0.0395	0.0286	1.3811	−0.0109
$SiAl_3^-$–ClOH-**4**		0.0358	0.0392	−0.0217	0.0157	1.3822	−0.0060
$GeAl_3^-$–ClOH-**1**		0.0588	0.0574	−0.0482	0.0313	1.5399	−0.0169
$SnAl_3^-$–ClOH-**1**		0.0602	0.0281	−0.0424	0.0247	1.7166	−0.0177
$PbAl_3^-$–ClOH-**1**		0.0573	0.0528	−0.0411	0.0272	1.5110	−0.0139
$SiAl_3^-$–ClOH-**1**	O···Cl	0.1024	0.1652	−0.1088	0.0750	1.4507	−0.0338
$SiAl_3^-$–ClOH-**2**		0.1005	0.1720	−0.1068	0.0749	1.4259	−0.0319
$SiAl_3^-$–ClOH-**3**		0.1004	0.1703	−0.1064	0.0745	1.4282	−0.0319
$SiAl_3^-$–ClOH-**4**		0.1095	0.1680	−0.1195	0.0808	1.4790	−0.0387
$GeAl_3^-$–ClOH-**1**		0.1023	0.1661	−0.1087	0.0751	1.4474	−0.0336
$SnAl_3^-$–ClOH-**1**		0.1003	0.1374	−0.1024	0.0684	1.4971	−0.0340
$PbAl_3^-$–ClOH-**1**		0.0982	0.1243	−0.0958	0.0634	1.5110	−0.0324

and $GeAl_3^-$–$BrCF_3$-**1** complexes have $H_b < 0$ and $1 < |V_b|/G_b < 2$, implying that these halogen bonds belong to the closed-shell interaction; however, out of those with $H_b > 0$ (<0.0006 a.u.), the others have $|V_b|/G_b < 1$ and thus belong to pure closed-shell interaction. In a word, the strength of halogen bonds increases and the contribution of orbital interaction to the formation of halogen bonds increases gradually in the order of X = Cl < Br < I. For the HOX-containing complexes, the values of ρ_b are relatively larger than those of the HCCX- and F_3CX-containing complexes and beyond the range of 0.002–0.035 a.u. In addition, except for $SiAl_3^-$–XOH-**1**, $SiAl_3^-$–IOH-**2** and $SiAl_3^-$–IOH-**3** complexes, the $\nabla^2\rho_b$ values of HOCl-containing complexes are positive and H_b values are negative, which indicate that these Cl···M/O interactions are partially covalent. But complexes $SiAl_3^-$–XOH-**1**, $SiAl_3^-$–IOH-**2** and $SiAl_3^-$–IOH-**3** correspond to a short bond lengths of Si/Al–Cl, large interaction energies ΔE^{cp}, negative $\nabla^2\rho_b$ and H_b, implying that the Si/Al atoms have formed new covalent bonds with X atoms in these complexes. Bond order is an important concept for understanding the nature of a chemical bond. Laplacian bond order [52] is defined as a scaled integral of negative parts of the Laplacian of electron density in fuzzy overlap space. Moreover, the Laplacian bond orders of C–Cl in HCCCl and F_3CCl and O–Cl in HOCl are 1.28 and 1.01 and 0.29, respectively, indicating that the O–Cl bond in HOCl is much weaker than the C–Cl bond in HCCCl and F_3CCl. This can well explain the breakage of O–Cl bond and the formation of a new Al/M–Cl bond. It is also responsible for the different arrangements and interaction nature in HOX-containing complexes.

The Laplacian bond orders for M-Cl, C–Cl and O–Cl bonds in the Cl complexes are listed in Table 4. The HCCCl- and F_3CCl-containing complexes with traditional halogen bonds have small bond orders (~0.01) for the M–Cl bonds, and the C–Cl bond orders are >1.00. These indicate that the influence of these weak interactions on the C–Cl bonds is negligible. By contrast, the Si–Cl bond order is 0.19 and the O–Cl bond order is 0.08 in complex $SiAl_3^-$–ClOH-**1**. In the other $SiAl_3^-$–ClOH complex with

Table 4 Laplacian bond orders for the M–Cl (M = Al, Si, Ge, Sn, Pb), C–Cl and O–Cl bonds in the Cl complexes

Complex	Y = HCC–		Y = F_3C–		Y = HO–	
	M–Cl	C–Cl[a]	M–Cl	C–Cl[b]	M–Cl	O–Cl[c]
$SiAl_3^-$–ClY-**1**	0.01	1.29	0.01	1.09	0.19	0.08
$SiAl_3^-$–ClY-**2**	0.01	1.30	0.01	1.09	0.11	0.08
$SiAl_3^-$–ClY-**3**	0.01	1.29	0.00	1.07	0.11	0.08
$SiAl_3^-$–ClY-**4**	0.00	1.30	0.00	1.07	0.01	0.08
$GeAl_3^-$–ClY-**1**	0.00	1.29	0.00	1.08	0.06	0.07
$SnAl_3^-$–ClY-**1**	0.01	1.29	0.01	1.07	0.09	0.07
$PbAl_3^-$–ClY-**1**	0.01	1.29	0.01	1.08	0.09	0.06

[a] Bond order in HCCCl is 1.28. [b] Bond order in F_3CCl is 1.01. [c] Bond order in HOCl is 0.29

chlorine-shared halogen bonds, the M-Cl bond orders are similar to those of O–Cl bonds. The geometries, interaction energies, NBO analysis and Laplacian bond orders of $SiAl_3^-$–ClOH complexes with chlorine-shared halogen bonds suggest that these strong interactions weaken the O–Cl bond and make the M–Cl interaction having the character of a covalent bond.

3.1.3 ELF analysis

To intuitively understand the difference in interaction strength in complexes $SiAl_3^-$–ClCCH, $SiAl_3^-$–$ClCF_3$ and $SiAl_3^-$–ClOH, ELF analysis for complexes $SiAl_3^-$–ClCCH-**1**, $SiAl_3^-$–$ClCF_3$-**1**, $SiAl_3^-$–ClOH-**1** and $SiAl_3^-$–ClOH-**2** was further performed, as shown in Fig. 5. All the values of ELF are within the range of 0–1.0. A large ELF value indicates that the electron is greatly localized in that area, implying a covalent bond, a lone pair or inner shells of an atom. As shown in Fig. 5, the electron localization regions are divided into two separate parts for complexes $SiAl_3^-$–ClCCH-**1** and $SiAl_3^-$–$ClCF_3$-**2**, which indicates that the halogen bonds are mainly electrostatic interaction (pure closed-shell interaction). However, for $SiAl_3^-$–ClOH-**1** and $SiAl_3^-$–ClOH-**2** complexes, the electron localization areas have been linked together. The ELF value between Si and Cl atoms is large in $SiAl_3^-$–ClOH-1 complex, implying the bond Si–Cl being a covalent bond. However, the ELF value of Al and Cl atoms in complex $SiAl_3^-$–ClOH-2 is relatively small, indicating that the halogen bond is partially covalent and belongs to chlorine-shared halogen bond. At the same time, ELF value between O and Cl atoms is ~0.35, implying the interaction between O and Cl atoms in complexes $SiAl_3^-$–ClOH possesses some covalent properties. These are fully consistent with the results of AIM analysis.

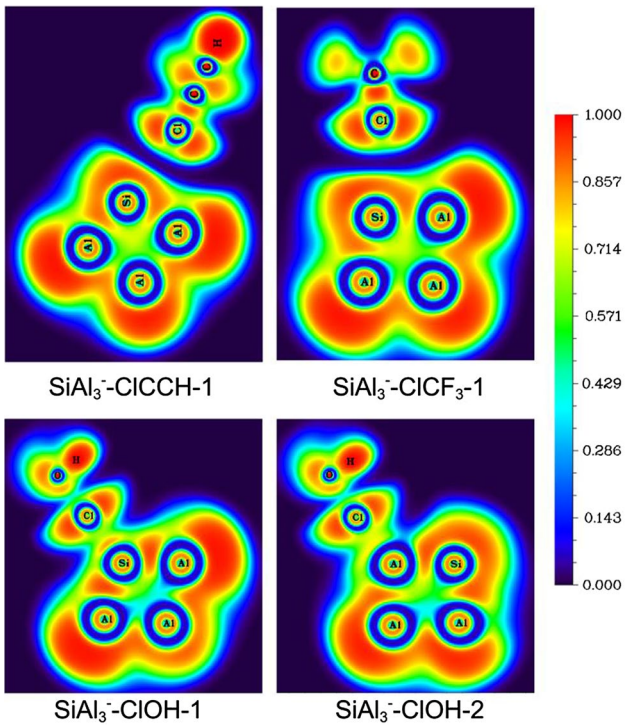

Fig. 5 Representation of electron localization function (ELF) for complexes $SiAl_3^-$–ClCCH-**1**, $SiAl_3^-$–$ClCF_3$-**1**, $SiAl_3^-$–ClOH-**1** and $SiAl_3^-$–ClOH-**2**

4 Hydrogen bond

For hypohalous acids (HOX, X = Cl, Br, I), both the H and the X atoms have one most positive electrostatic potential site. The H atom can form a hydrogen bond with Lewis base, and the X atom can form a halogen bond. In the previous studies of HOCl-containing complexes [28, 29, 53, 54], it is found that the hydrogen-bonded complex is more stable than the halogen-bonded complex. To compare the strengths of hydrogen bonds and halogen bonds, four types of hydrogen-bonded complexes of HOCl and $SiAl_3^-$ are optimized, which are shown in Figure S3 (top). We found that these hydrogen-bonded complexes exhibit similar arrangements with the halogen-bonded complexes of HCCCl and $SiAl_3^-$. Frequency calculations reveal that the complex $SiAl_3^-$–HOCl-**1** corresponds to a very small imaginary frequency (~10*i*). Table S8 presents the bond

lengths (R), changes in H–O bond lengths and BSSE-corrected interaction energies of hydrogen-bonded complexes $SiAl_3^-$–HOCl. Although the bond lengths (R) in hydrogen-bonded complexes $SiAl_3^-$–HOCl are similar to those of halogen-bonded complexes $SiAl_3^-$–ClOH, ΔE^{cp} of halogen-bonded complexes are about two times as much as those of hydrogen-bonded complexes. The molecular graphs of complexes $SiAl_3^-$–HOCl are shown in Figure S3 (bottom). One can see that BCPs between the H and Si/Al atoms and the bond paths connecting the H and Si/Al atoms are present, which indicate the existence of hydrogen bonds in complexes $SiAl_3^-$–HOCl. Tables S8 and S9 show that the stabilization energies of the orbital interaction are larger than corresponding interaction energies. Although the stabilization energies have no direct correlation with the interaction energies, the orbital interactions may also play an important role in forming halogen bonds in the complexes $SiAl_3^-$–HOCl. Because the interaction energy may be perturbed by a repulsive term, NBO analysis could not provide the value of repulsive interaction. The BCPs properties of these hydrogen-bonded complexes are listed in Table S10. All hydrogen-bonded complexes have $\nabla^2\rho_b > 0$, $H_b < 0$ and $1 < |V_b|/G_b < 2$. AIM analysis shows that the interactions in these hydrogen-bonded complexes are closed-shell interactions with partial covalent characteristic. NBO analysis indicated that, in the complexes formed by $SiAl_3^-$ and HOCl, the hydrogen and halogen bonds display different nature, i.e., in the hydrogen-bonded complexes, the original O–H bonds in the monomers of HOX are still kept, but in the halogen-bonded complexes, the original O–Cl bonds have been broken and new Al/M-Cl bonds have been formed.

5 Conclusions

In this paper, the structures, properties and nature of unconventional halogen-bonded complexes between doped all-metal aromatic clusters MAl_3^- (X = Si, Ge, Sn, Pb) and YX (Y = HCC–, F_3C–, HO–; X = Cl, Br, I) have been explored at the MP2/aug-cc-pVTZ level. Our calculations reveal that four types of interaction modes of halogen-bonded complexes are found between $SiAl_3^-$ and YX (Y = HCC–, F_3C–, HO–; X = Cl, Br, I). But the arrangements of configurations **2** and **3** of HOX-containing complexes are different from those of HCCX- and F_3CX-containing complexes. Although the most positive electrostatic potentials of Cl atoms in the three monomers YCl are similar, the interaction strengths of halogen bonds in the HOCl-containing complexes are about four times as those in the HCCCl- and F_3CCl-containing complexes. When X is I atom, the most positive electrostatic potential on the surface of I atom in HOI is larger than those of HCCI and F_3CI. However, the interaction strengths of HOI-containing complexes are about two times as those of HCCI- and F_3CI-containing complexes. With the increase in X atomic mass number, the interaction energy increases gradually for the same type of halogen-bonded complexes. For the HCCX- and F_3CX-containing complexes, the doped M atoms have minor influence on their structures and interaction strengths, which is different from the HOX-containing complexes that the influence of doped M atoms on the interaction strength is great. NBO, AIM and ELF analyses indicate that, for HCCX- and F_3CX-containing complexes, the electrostatic interaction plays a dominant role in the formation of halogen bonds in the Cl complexes and some Br complexes. Therefore, the orbital interaction plays a more important role in the formation of halogen bonds in the other Br and I complexes. In a word, with the increase in X atomic number, the covalent character of halogen bonds is increased in HCCX- and F_3CX-containing complexes. Besides, the Cl–M/Al bonds in complexes $SiAl_3^-$–HOX-**1**, $SiAl_3^-$–HOI-**2** and $SiAl_3^-$–HOI-**3** belong to covalent bonds, and the halogen bonds of Cl–M/Al in the other complexes of $SiAl_3^-$–HOX have partial covalent character and are halogen-shared halogen bonds. With regard to complexes formed by $SiAl_3^-$ and HOCl, the halogen-bonded complexes are more stable than the hydrogen-bonded complexes. The difference between HOX-containing complexes and other complexes may be the result of the special O–X (X = Cl, Br, I) bonds in HOX, which are of donor–acceptor type with halogen atom donating its electron density to the oxygen valence shell.

Acknowledgments This work was supported by the Natural Science Foundation of China (21373125, 21573127).

References

1. Konold P, Regmi CK, Chapagain PP, Gerstman BS, Jimenez R (2014) J Phys Chem B 118:2940–2948
2. Aboaku S, Paduan-Filho A, Bindilatti V, Oliveira NF Jr, Schlueter JA, Lahti PM (2011) Chem Mater 23:4844–4856
3. Xue C, Jin S, Weng X, Ge JJ, Shen Z, Shen H, Graham MJ, Jeong K-U, Huang H, Zhang D, Guo M, Harris FW, Cheng SZD, Li CY, Zhu L (2004) Chem Mater 16:1014–1025
4. Troff RW, Mäkelä T, Topić F, Valkonen A, Raatikainen K, Rissanen K (2013) Eur J Org Chem 9:1617–1637
5. Scholfield MR, Vander Zanden CM, Carter M, Shing Ho P (2013) Protein Sci 22:139–152
6. Priimagi A, Cavallo G, Metrangolo P, Resnati G (2013) Acc Chem Res 46:2686–2695
7. Politzer P, Murray JS, Clark T (2010) Phys Chem Chem Phys 12:7748–7757
8. Legon AC (1999) Angew Chem Int Ed 38:2686–2714
9. Legon AC (2010) Phys Chem Chem Phys 12:7736–7747
10. Shields ZP, Murray JS, Politzer P (2010) Int J Quantum Chem 110:2823–2832
11. Bent HA (1968) Chem Rev 68:587–648

12. Hassel O (1970) Science 170:497–502
13. Koskinen L, Jääskeläinen S, Hirva P, Haukka M (2015) Gryst Growth Des 15:1160–1167
14. Grabowski SJ (2013) Theor Chem Acc 132:1347
15. Li QZ, Li R, Liu XF, Li WZ, Cheng JB (2012) ChemPhysChem 13:1205–1212
16. Politzer P, Murray JS (2013) ChemPhysChem 14:278–294
17. Feng G, Evangelisti L, Gasparini N, Caminati W (2012) Chem Eur J 18:1364–1368
18. Politzer P, Murray JS, Clark T (2013) Phys Chem Chem Phys 15:11178–11189
19. Saraswatula VG, Saha BK (2014) New J Chem 38:897–901
20. Politzer P, Murray JS (2012) Theor Chem Acc 131:1114
21. Stone AJ (2013) J Am Chem Soc 135:7005–7009
22. Jahromi HJ, Eskandari K, Alizadeh A (2015) J Mol Model 21:112
23. Wu WH, Lu YX, Liu YT, Li HY, Peng CJ, Liu HL, Zhu WL (2013) Chem Phys Lett 582:49–55
24. Zhao Q (2014) J Mol Model 20:2458
25. Grabowski SJ (2014) Chem Phys Lett 605:131–136
26. Wang WZ (2011) J Phys Chem A 115:9294–9299
27. Berski S, Silvi B, Latajka Z, Leszczyński J (1999) J Chem Phys 111:2542–2555
28. Blanco F, Alkorta I, Solimannejad M, Elguero J (2009) J Phys Chem A 113:3237–3244
29. Li QZ, Xu XS, Liu T, Jing B, Li WZ, Cheng JB, Gong BA, Sun JZ (2010) Phys Chem Chem Phys 12:6837–6843
30. Li XW, Pennington WT, Robinson GH (1995) J Am Chem Soc 117:7578–7579
31. Li X, Kuznetsov AE, Zhang HF, Boldyrev AI, Wang LS (2001) Science 291:859–861
32. Li R, Li QZ, Cheng JB, Li WZ (2012) J Mol Model 18:2311–2319
33. Li X, Zhang HF, Wang LS, Kuznetsov AE, Cannon NA, Boldyrev AI (2001) Angew Chem Int Ed 40:1867–1870
34. Grabowski SJ (2004) J Phys Org Chem 17:18–31
35. Frisch MJ, Trucks GW, Schlegel HB, Scuseria GE, Robb MA, Cheeseman JR, Scalmani G, Barone V, Mennucci B, Petersson GA et al. (2009) Gaussian 09, Revision B.01, Gaussian, Inc., Wallingford, CT
36. Samanta PN, Das KK (2012) Comput Theor Chem 1000:42–51
37. Peterson KA (2003) J Chem Phys 119:11099–11112
38. Boys SF, Bernardi F (1970) Mol Phys 19:553–566
39. Reed AF, Curtiss LA, Weinhold F (1988) Chem Rev 88:899–926
40. Bader RFW (1990) Atoms in molecules, a quantum theory. Oxford University Press, Oxford
41. AIMAll, Version 12.06.03; Todd A. Keith, TK Gristmill Software, Overland Park, KS, USA, 2012; aim.tkgristmill.com
42. Lu T, Chen FW (2012) J Comput Chem 33:580–592
43. Lu T, Chen FW (2012) J Mol Graph Model 38:314–323
44. Alkorta I, Elguero J (2014) J Phys Chem A 118:4222–4231
45. Li QZ, Li R, Liu XF, Li WZ, Cheng JBP (2012) J Phys Chem A 116:2547–2553
46. Grabowski SJ (2012) J Phys Chem A 116:1838–1845
47. Alikhani ME, Fuster F, Silvi B (2005) Struct Chem 16:203–210
48. Lu YX, Zou JW, Wang YH, Jiang YJ, Yu QS (2007) J Phys Chem A 111:10781–10788
49. Cremer D, Kraka E (1984) Angew Chem Int Ed Engl 23:627–628
50. Jenkins S, Morrison I (2000) Chem Phys Lett 317:97–102
51. Koch U, Popelier PLA (1995) J Phys Chem A 99:9747–9754
52. Lu T, Chen FW (2013) J Phys Chem A 117:3100–3108
53. Alkorta I, Blanco F, Solimannejad M, Elguero J (2008) J Phys Chem A 112:10856–10863
54. Li QZ, Li H, Gong JH, Li WZ, Cheng JB (2012) Int J Quantum Chem 112:2429–2434